

Elastic properties of Janus transition metal dichalcogenide nanotubes from first principles

Arpit Bhardwaj and Phanish Suryanarayana*

College of Engineering, Georgia Institute of Technology, Atlanta, GA 30332, USA

Abstract

We calculate the elastic properties of Janus transition metal dichalcogenide (TMD) nanotubes using first principles Kohn-Sham density functional theory (DFT). Specifically, we perform electronic structure simulations that exploit the cyclic and helical symmetry in the system to compute the Young's moduli, Poisson's ratios, and torsional moduli for twenty-seven select armchair and zigzag Janus TMD nanotubes at their equilibrium diameters. We find the following trend in the moduli values: $MSSe > MSTe > MSeTe$, while their anisotropy with respect to armchair and zigzag configurations has the following ordering: $MSTe > MSeTe > MSSe$. This anisotropy and its ordering between the different groups is confirmed by computing the shear modulus from the torsional modulus using an isotropic elastic continuum model, and comparing it against the value predicted from the isotropic relation featuring the Young's modulus and Poisson's ratio. We also develop a model for the Young's and torsional moduli of Janus TMD nanotubes based on linear regression.

I. INTRODUCTION

Nanotubes are tubular structures with diameters that typically range from one to few tens of nanometers. They have been the subject of a number of research efforts, motivated by their enhanced/novel mechanical, electronic, thermal, and optical properties, especially when compared to their bulk counterparts¹⁻³. In particular, since the landmark realization of carbon nanotubes in the year 1991⁴, more than thirty distinct nanotubes have been synthesized, with many more likely in the future. This is because nanotubes can be constructed from their two-dimensional counterparts (atleast in concept), thousands of which have been predicted to be stable⁵⁻⁷ from first principles Kohn-Sham density functional theory (DFT)^{8,9} calculations.

Transition metal dichalcogenide (TMD) nanotubes — one-dimensional analogues of the two-dimensional materials of the form MX_2 , where M and X are used to represent the transition metal and chalcogen, respectively — are currently the most varied group, with the highest number of materials synthesized to date¹⁻³. In particular, they are known for their large tensile strength¹⁰⁻¹⁴ and electronic properties that can be tuned through mechanical deformations¹⁵⁻²². However, most of these nanotubes are multi-walled and have large diameters, which limits the appearance of novel and exotic properties found in small diameter single-walled nanotubes susceptible to quantum confinement effects. Furthermore, only a small fraction of the total number of possible TMD nanotubes have been synthesized to date, which can be partly attributed to the relatively high bending energy associated with TMD nanotubes²³.

The recent synthesis of Janus TMD monolayers²⁴⁻²⁷ — materials of the form MXY , where X and Y represent different chalcogens — presents an opportunity to overcome some of the aforementioned limitations of TMD nanotubes. In particular, the asymmetry introduced by having different chalcogens on either side of the monolayer makes the nanotube configuration more energetically favorable²⁸, likely making them easier to synthesize, particularly given that there exists an energy minimizing nanotube diameter. This has motivated a number of studies for predicting the electronic^{16,29-33} and optical^{16,30,34-37} properties of Janus TMD nanotubes from first principles DFT calculations. Janus TMD nanotubes are ex-

pected to have a number of technological applications, including optoelectric^{16,30,37,38} and nanoelectromechanical (NEMS) devices^{21,45,46}, as well as nanocomposites reinforcement^{39–44}. In all cases, an accurate characterization of the elastic properties is important for the design process. However, apart from Ref.²⁹ where the Young’s modulus of the MoSSe nanotube has been computed using DFT, the mechanical properties of Janus TMD nanotubes remain unexplored heretofore.

In this work, we compute the elastic properties of single-walled Janus TMD nanotubes from first principles. Specifically, considering the zigzag and armchair versions of the twenty-seven Janus TMD nanotube that have previously been predicted to be stable, we calculate the Young’s moduli, Poisson’s ratios, and torsional moduli for these materials at their equilibrium diameters, all using cyclic and helical symmetry-adapted Kohn-Sham DFT. We find the following trend in the moduli: MSSe > MSTe > MSeTe, while their anisotropy with respect to armchair and zigzag configurations has the following ordering: MSTe > MSeTe > MSSe. This anisotropy and its ordering between the different groups is confirmed by computing the shear modulus value from the torsional modulus using an isotropic elastic continuum model, and comparing it with that predicted by the isotropic relation featuring the Young’s modulus and Poisson’s ratio. We also develop a model for the Young’s and torsional moduli of the nanotubes based on linear regression, with the following features: metal-chalcogen bonds’ nature/characteristics and the difference in electronegativity between the chalcogens.

The remainder of this article is organized as follows. In Section II, we list the Janus TMD nanotubes selected and describe the calculation of their elastic properties using symmetry-adapted Kohn-Sham DFT simulations. The results so obtained are presented and discussed in Section III. Finally, we conclude in Section IV.

II. SYSTEMS AND METHODS

We consider twenty-seven materials that represents the set of all single-walled Janus TMD nanotubes that have previously been predicted to be stable⁴⁹. Specifically, we consider the following nanotubes: (i) $M=\{V, Nb, Ta, Cr, Mo, W\}$ and $X,Y=\{S, Se, Te\}$ with 2H-t symmetry^{47,48}, and (ii) $M=\{Ti, Zr, Hf\}$ and $X,Y=\{S, Se, Te\}$ with 1T-o symmetry^{47,48}, all

in both armchair and zigzag configurations, with the heavier chalcogen on the outside. The diameters for these nanotubes are selected so as to minimize the ground state Kohn-Sham energy⁴⁹, since experimentally synthesized nanotubes are likely to adopt energy minimizing configurations.

We perform Kohn-Sham DFT simulations to calculate the elastic properties of the nanotubes using the Cyclix-DFT⁵⁰ feature in the state-of-the-art real-space code SPARC^{51–53}. In particular, Cyclix-DFT can exploit the cyclic and helical symmetry in the system to reduce all computations to the fundamental domain^{50,54,55}, which in the current context is a unit cell with only 3 atoms: 1 metal atom and 1 chalcogen atom of each type, a situation that is true even on the application of axial and/or torsional deformations (Fig. 1). This symmetry-adaptation provides tremendous reduction in the computational expense, with many of the simulations performed here impractical for even state-of-the-art DFT codes, even on powerful supercomputers^{51,56}. For instance, a MoSSe nanotube of diameter ~ 8.5 nm subject to a twist of 6×10^{-4} rad/Bohr has 219,888 atoms in the unit cell when traditional periodic boundary conditions are prescribed, a system that is clearly intractable using standard approaches. Note that the accuracy of Cyclix-DFT has been verified by not only comparison with established DFT codes⁵⁰, but also through its ability to make accurate predictions in a number of physical applications^{14,22,23,57,58}.

In all the simulations, we employ pseudopotentials from the SPMS collection⁶⁰, which is a set of transferable and soft optimized norm-conserving Vanderbilt (ONCV) pseudopotentials⁶¹ with nonlinear core correction (NLCC). The accuracy of the pseudopotentials in the current context is confirmed by the very good agreement of the computed equilibrium geometry (Supplementary Material) with previous DFT results for Janus TMD nanotubes^{29–32,49} as well as monolayers^{7,33,49,62}. We employ the semilocal Perdew–Burke–Ernzerhof (PBE) exchange–correlation functional⁶³, which is considered to accurately describe properties/behavior for TMD systems^{5,7,17,29–33,49,62,64–69}, as validated by experimental measurements^{24,25,47,70–77}. Indeed, the use of more advanced density functionals such as hybrids and/or inclusion of spin orbit coupling (SOC) are not expected to change the elastic properties noticeably, given that small strains are accompanied by small perturbations of electron density with respect to the undeformed nanotube, which translates to significant cancellations of error while taking

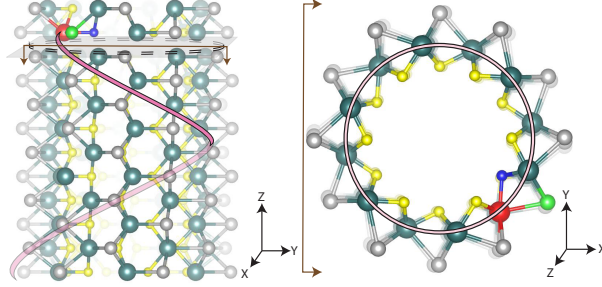


Figure 1: Illustration of a twisted (6,6) TMD Janus nanotube with 2H-t symmetry, generated using VESTA⁵⁹. In particular, every atom in the nanotube is a cyclic and/or helical image of one of the three fundamental domain atoms: the metal and chalcogen atoms colored red and blue/green, respectively. This cyclic and helical symmetry is exploited while performing Kohn-Sham simulations using the Cyclix-DFT feature⁵⁰ in the SPARC code^{51–53}.

energy differences. This is expected to be particularly true in the current context, given that the difference between PBE and hybrid functionals for calculating ground state electron density has been found to be relatively small for TMD monolayers, both with and without SOC²³.

We calculate the Young’s modulus E , Poisson’s ratio ν , and torsional modulus K by fitting the data to the relations:

$$\mathcal{E}(0, \varepsilon, \tilde{\varepsilon}^*(\varepsilon)) \equiv \min_{\tilde{\varepsilon}} \mathcal{E}(0, \varepsilon, \tilde{\varepsilon}) = \mathcal{E}(0, 0, 0) + \frac{1}{2} E \varepsilon^2, \quad (1)$$

$$\tilde{\varepsilon}^* = -\nu \varepsilon, \quad (2)$$

$$\mathcal{E}(\theta, \varepsilon^*(\theta), 0) \equiv \min_{\varepsilon} \mathcal{E}(\theta, \varepsilon, 0) = \mathcal{E}(0, 0, 0) + \frac{1}{2} K \theta^2, \quad (3)$$

where $\mathcal{E}(\theta, \varepsilon, \tilde{\varepsilon})$ is the energy density — value at the electronic ground state corresponding to the force-relaxed atomic configuration — for twist density θ , axial strain ε , and circumferential/hoop strain $\tilde{\varepsilon}$, with both energy and twist densities defined to be per unit length of the nanotube. The superscript * is used to denote the value of the quantity that minimizes the energy density. The numerical parameters in the Cyclix-DFT simulations, including real-space grid spacing, reciprocal space grid spacing for Brillouin zone integration, radial vacuum, and cell/atom structural relaxation tolerances are selected to ensure

that the reported Young’s and torsional moduli are converged to within 1% of their values. This translates to the ground state energy being accurate to within 10^{-5} Ha/atom, which is required to capture the exceedingly small energy differences that exist for the mechanical deformations considered in this work, which have been chosen to be small enough so as to have strains are in accordance with those used in experiments.^{11,12,21,46,78}

III. RESULTS AND DISCUSSION

We have performed the aforescribed symmetry-adapted Kohn-Sham DFT simulations to calculate the elastic properties of the twenty-seven select Janus TMD nanotubes, in both armchair and zigzag configurations, at their equilibrium diameters. The results so obtained have been summarized in Table I and Fig. 2, which we discuss in detail below. All simulation data can be found in the Supplementary Material. Note that the results for the torsional moduli are reported in terms of the diameter-independent quantity referred to as the torsional modulus coefficient $\hat{k} = K/d^{314}$, where d is the nanotube diameter. Also note that both the Young’s and torsional moduli are reported in units of N/m rather than N/m², since the latter requires an assumption on the thickness of the nanotube, whose value is not clearly defined⁷⁹.

The equilibrium radii generally follow the trend: MSTe < MSeTe < MSSe, which can be correlated to the difference in electronegativity between the chalcogens, i.e., larger electronegativity differences result in smaller equilibrium diameters, an observation that is in agreement with previous DFT results for M={Nb, Ta, Mo, W} and X,Y={S, Se, Te}³³. The computed equilibrium diameters for these systems are also in excellent agreement with Ref³³, the maximum difference being 0.4 nm, which occurs for NbSSe. In terms of comparison with Ref.⁴⁹, which also employs DFT to predict the equilibrium diameters for all the materials studied here, while there is good agreement for nanotubes with smaller diameters, the difference increases with nanotube diameter, reaching a maximum of 22.8 nm for TiSeTe. This is a consequence of Ref.⁴⁹ using extrapolation from the data for small diameters — the current work employs interpolation, with data points on either side of the equilibrium diameter—whereby larger errors are accumulated when the equilibrium diameter is farther away from

Table I: Young's modulus (E), Poisson's ratio (ν), and torsional modulus coefficient (\hat{k}) for the twenty-seven select Janus TMD nanotubes from Kohn-Sham DFT calculations.

M	MSSe							
	Armchair				Zigzag			
	D (nm)	E (N/m)	ν	\hat{k} (N/m)	D (nm)	E (N/m)	ν	\hat{k} (N/m)
W	8.8 ± 0.5	106	0.25	39	9.0 ± 0.5	114	0.19	38
Mo	8.4 ± 0.2	96	0.28	33	8.3 ± 0.1	104	0.22	33
Cr	7.2 ± 0.3	87	0.35	30	7.5 ± 0.4	97	0.25	29
Ta	11.1 ± 1.5	80	0.41	25	11.2 ± 1.5	90	0.29	25
V	14.6 ± 2	72	0.32	23	14.2 ± 2.3	79	0.24	27
Nb	13.1 ± 1.4	68	0.35	23	14.1 ± 1.4	76	0.26	23
Hf	9.5 ± 0.5	62	0.20	22	10.4 ± 0.5	65	0.15	22
Zr	15.5 ± 3	57	0.19	20	14.9 ± 2.4	59	0.14	20
Ti	43.9 ± 5.9	60	0.21	19	44.9 ± 4.9	62	0.20	20
M	MSTe							
	Armchair				Zigzag			
	D (nm)	E (N/m)	ν	\hat{k} (N/m)	D (nm)	E (N/m)	ν	\hat{k} (N/m)
W	3.8 ± 0.1	80	0.42	32	3.8 ± 0.1	99	0.31	35
Mo	3.8 ± 0.1	74	0.48	28	3.8 ± 0.1	93	0.40	30
Cr	3.1 ± 0.1	60	0.54	22	3.1 ± 0.1	83	0.36	25
Ta	4.0 ± 0.1	65	0.53	24	4.1 ± 0.06	80	0.42	28
V	4.4	48	0.43	21	4.4 ± 0.06	65	0.47	21
Nb	4.4 ± 0.1	47	0.55	23	4.4 ± 0.1	69	0.39	20
Hf	4.4 ± 0.4	43	0.30	19	4.4 ± 0.4	51	0.24	18
Zr	6.1 ± 0.2	39	0.29	16	6.1 ± 0.2	45	0.20	15
Ti	10.0 ± 0.4	46	0.34	16	9.7 ± 0.6	48	0.34	14
M	MSeTe							
	Armchair				Zigzag			
	D (nm)	E (N/m)	ν	\hat{k} (N/m)	D (nm)	E (N/m)	ν	\hat{k} (N/m)
W	6.7 ± 0.1	77	0.26	31	7.1 ± 0.1	85	0.18	31
Mo	6.6 ± 0.3	69	0.32	27	6.5 ± 0.3	81	0.19	27
Cr	5.6 ± 0.2	62	0.44	22	5.6 ± 0.1	73	0.34	22
Ta	7.6 ± 0.3	58	0.40	20	7.6 ± 0.2	66	0.31	20
V	8.4 ± 0.6	52	0.38	17	8.2 ± 0.5	59	0.27	25
Nb	8.7 ± 0.8	53	0.38	18	8.9 ± 0.8	59	0.28	16
Hf	8.2 ± 0.5	40	0.15	17	8.1 ± 0.6	44	0.10	16
Zr	16.6 ± 3	38	0.20	14	15.8 ± 2.2	42	0.12	14
Ti	39.3 ± 10.9	41	0.16	13	28.7 ± 4.9	40	0.15	13

the region where Kohn-Sham calculations have actually been performed.

We observe from the results that the Young's moduli and torsional modulus coefficients

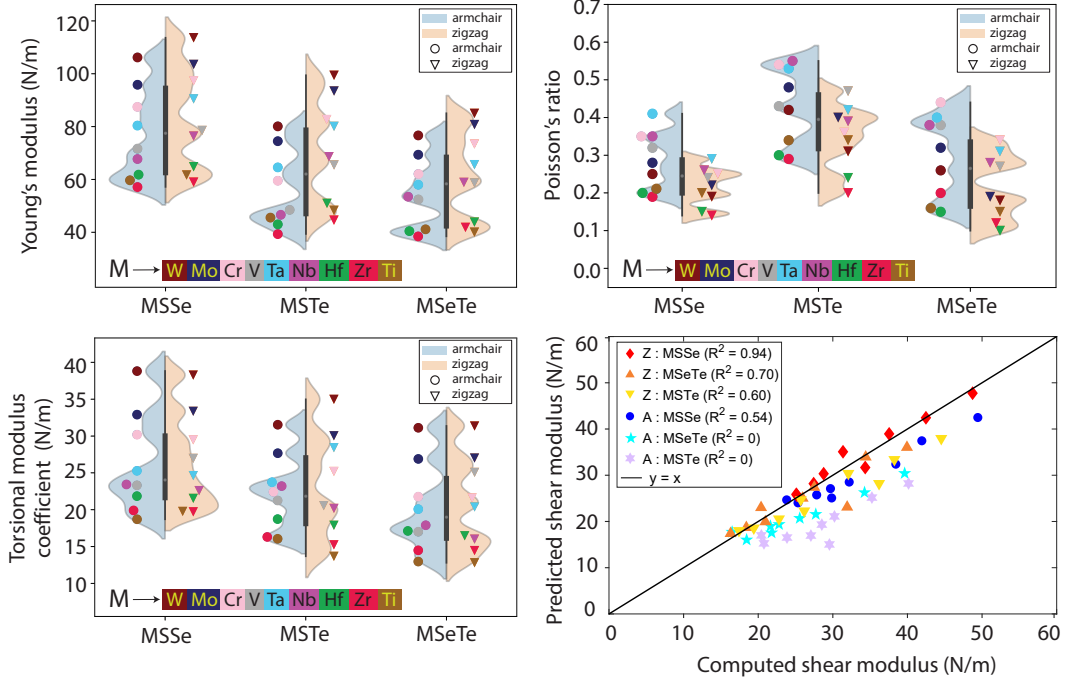


Figure 2: Young’s modulus (E), Poisson’s ratio (ν), and torsional modulus coefficient (\hat{k}) for the twenty-seven select armchair and zigzag Janus TMD nanotubes. Also shown is the shear modulus computed from the torsional modulus coefficient vs. that predicted from the Young’s modulus and Poisson’s ratio. The R^2 values listed in the legend represent the linear regression’s coefficient of determination.

for the Janus TMD nanotubes lie between the corresponding values for the parent TMD nanotubes¹⁴. In addition, we find that they follow the trend: $\text{MSSe} > \text{MSTe} > \text{MSeTe}$, which is the reverse of that for the metal-chalcogen bond lengths. Indeed, increased overlap of the orbitals at shorter interatomic distances is expected to result in stronger bonds. In terms of individual values, WSSe and ZrSeTe have the largest and smallest Young’s moduli, respectively, while WSSe and TiSeTe have the largest and smallest torsional modulus coefficients, respectively. Notably, carbon nanotube’s moduli ($E = 345 \text{ N/m}^{80}$ and $\hat{k} = 117 \text{ N/m}^{50}$) are close to a factor of three higher than the largest values here, a likely consequence of the very strong covalent carbon-carbon bonds. Regarding the Poisson’s ratio, we find that the armchair CrSTe, TaSTe, NbSTe nanotubes have values larger than 0.5 — theoretical limit for isotropic materials⁸¹ — which suggests their anisotropic nature, a result that we

further confirm below. Note that we are not aware of any theoretical or experimental results in literature against which we can compare the values reported in this work. Indeed, the predictions made for MoSSe in Ref.²⁹ cannot be compared, given the significantly smaller diameter chosen there compared to the equilibrium value used here.

We also observe from the results that anisotropy with respect to armchair and zigzag configurations follows the ordering: $\text{MSTe} > \text{MSeTe} > \text{MSSe}$, which can likely be attributed to the level of dissimilarity between the chalcogens. To confirm this, we compute the effective shear modulus using the relation $G = 4\hat{k}/\pi$ — corresponds to the nanotube being modeled as a homogeneous circular tube made of isotropic material, subject to an external twist — and compare it against that predicted by the relation featuring the Young’s modulus and Poisson’s ratio for isotropic materials: $G = E/2(1 + \nu)$. The results so obtained are summarized in Fig. 2, from which it is clear that the disagreement between the computed and predicted shear moduli follows the same trend as that stated above for the difference in values between armchair and zigzag configurations, indicative of the relative degree of anisotropy between the different groups. In addition, the armchair nanotubes are significantly more anisotropic compared to their zigzag counterparts.

The aforescribed results suggest that the nature/strength of the metal-chalcogen bonds as well as the level of dissimilarity between the chalcogen atoms plays a significant role in determining the Young’s and torsional moduli of Janus TMD nanotubes. In view of this, we develop a regression model with the following features: metal-chalcogen bond lengths, difference in electronegativity between the chalcogens, and sum of the ionization potential and electron affinity for the metal and chalcogens, respectively. In particular, we carry out a linear regression on the computed Young’s moduli and torsional modulus coefficients, whose results are presented in Fig. 3. The fit is reasonably good, which confirms that the features chosen for our model do play a notable role in deciding the elastic properties for Janus TMD nanotubes. It is worth noting that we can further improve the quality of the fit by using a higher-order regression. However, this strategy comes with the possibility of overfitting, and therefore not adopted here.

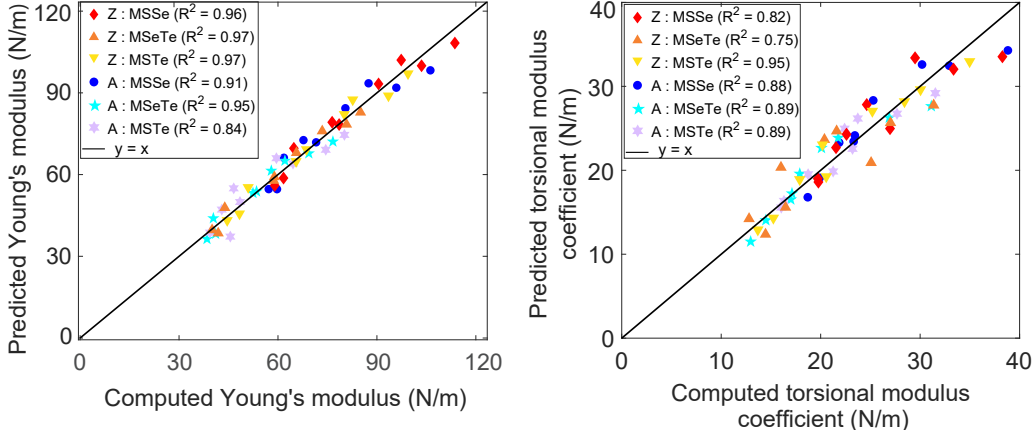


Figure 3: Computed Young's modulus and torsional modulus coefficient vs. that predicted by the model based on linear regression. The regression model has the following features: metal-chalcogen bond lengths, difference in electronegativity between the chalcogen atoms, and sum of ionization potential and electron affinity of metal and chalcogens respectively.

The R^2 values listed in the legend represent the linear regression's coefficient of determination.

IV. CONCLUDING REMARKS

In this work, we have calculated the elastic properties of select single-walled Janus TMD nanotubes from first principles Kohn-Sham DFT. In particular, considering the twenty-seven Janus TMD nanotubes that have previously been predicted to be stable, we have performed cyclic and helical symmetry-adapted electronic structure simulations to compute the Young's moduli, Poisson's ratios, and torsional moduli for the armchair and zigzag versions of these materials at their equilibrium diameters. We have found the following trend in the moduli: $MSSe > MSTe > MSeTe$, while their anisotropy with respect to armchair and zigzag configurations has the ordering: $MSTe > MSeTe > MSSe$. We have confirmed this anisotropy and ordering between the different groups by computing the shear modulus from the torsional modulus using an isotropic elastic continuum model, and comparing it with the value predicted from the isotropic relation featuring Young's modulus and Poisson's ratio. We have also developed a reasonably accurate model for Young's and torsional moduli

of Janus TMD nanotubes based on linear regression, with the following features: metal-chalcogen bonds' nature/characteristics and the difference in electronegativity between the chalcogens.

The electronic response of Janus TMD nanotubes to mechanical deformations presents itself as an interesting research problem worthy of pursuit, having a number of potential applications in semiconductor devices. In addition, given their anisotropic nature, the effect of chirality on the electromechanical response of Janus TMD nanotubes is also a worthy subject for future research.

ACKNOWLEDGEMENTS

The authors gratefully acknowledge the support of the US National Science Foundation (CAREER-1553212 and MRI-1828187).

* phanish.suryanarayana@ce.gatech.edu

- ¹ R Tenne. Advances in the synthesis of inorganic nanotubes and fullerene-like nanoparticles. *Angewandte Chemie International Edition*, 42(42):5124–5132, 2003.
- ² C N R Rao and M Nath. Inorganic nanotubes. In *Advances In Chemistry: A Selection of CNR Rao's Publications (1994–2003)*, pages 310–333. World Scientific, 2003.
- ³ M Serra, R Arenal, and R Tenne. An overview of the recent advances in inorganic nanotubes. *Nanoscale*, 11(17):8073–8090, 2019.
- ⁴ S Iijima. Helical microtubules of graphitic carbon. *Nature*, 354(6348):56–58, 1991.
- ⁵ J Zhou, L Shen, M D Costa, K A Persson, Shyue P Ong, P Huck, Y Lu, X Ma, Y Chen, H Tang, et al. 2DMatPedia, an open computational database of two-dimensional materials from top-down and bottom-up approaches. *Scientific Data*, 6(1):1–10, 2019.
- ⁶ M N Gjerding, A Taghizadeh, A Rasmussen, S Ali, F Bertoldo, T Deilmann, U P Holguin, N R Knøsgaard, M Kruse, S Manti, et al. Recent Progress of the Computational 2D Materials Database (C2DB). *2D Materials*, 8(4):044002, 2021.

- ⁷ S Hastrup, M Strange, M Pandey, T Deilmann, P S Schmidt, N F Hinsche, M N Gjerding, D Torelli, P M Larsen, A C Riis-Jensen, et al. The Computational 2D Materials Database: high-throughput modeling and discovery of atomically thin crystals. *2D Materials*, 5(4):042002, 2018.
- ⁸ W Kohn and L J Sham. Self-consistent equations including exchange and correlation effects. *Physical Review*, 140(4A):A1133, 1965.
- ⁹ P Hohenberg and W Kohn. Inhomogeneous electron gas. *Physical Review*, 136(3B):B864, 1964.
- ¹⁰ A Kis, D Mihailovic, M Remskar, A Mrzel, A Jesih, I Pivonski, A J Kulik, W Benoît, and L Forró. Shear and Young’s moduli of MoS₂ nanotube ropes. *Advanced Materials*, 15(9):733–736, 2003.
- ¹¹ I Kaplan-Ashiri and R Tenne. Mechanical properties of WS₂ nanotubes. *Journal of Cluster Science*, 18(3):549–563, 2007.
- ¹² I Kaplan-Ashiri, S R Cohen, K Gartsman, V Ivanovskaya, T Heine, G Seifert, I Wiesel, H D Wagner, and R Tenne. On the mechanical behavior of WS₂ nanotubes under axial tension and compression. *Proceedings of the National Academy of Sciences*, 103(3):523–528, 2006.
- ¹³ D-M Tang, X Wei, M-S Wang, N Kawamoto, Y Bando, C Zhi, M Mitome, A Zak, R Tenne, and D Golberg. Revealing the anomalous tensile properties of WS₂ nanotubes by in situ transmission electron microscopy. *Nano Letters*, 13(3):1034–1040, 2013.
- ¹⁴ A Bhardwaj, A Sharma, and P Suryanarayana. Torsional moduli of transition metal dichalcogenide nanotubes from first principles. *Nanotechnology*, 32(28):28LT02, 2021.
- ¹⁵ N Zibouche, M Ghorbani-Asl, T Heine, and A Kuc. Electromechanical properties of small transition-metal dichalcogenide nanotubes. *Inorganics*, 2(2):155–167, 2014.
- ¹⁶ S Oshima, M Toyoda, and S Saito. Geometrical and electronic properties of unstrained and strained transition metal dichalcogenide nanotubes. *Physical Review Materials*, 4(2):026004, 2020.
- ¹⁷ W Li, G Zhang, M Guo, and Y-W Zhang. Strain-tunable electronic and transport properties of MoS₂ nanotubes. *Nano Research*, 7(4):518–527, 2014.
- ¹⁸ M Ghorbani-Asl, N Zibouche, M Wahiduzzaman, A F Oliveira, A Kuc, and T Heine. Electromechanics in MoS₂ and WS₂: nanotubes vs. monolayers. *Scientific Reports*, 3:2961, 2013.

- ¹⁹ P Lu, X Wu, W Guo, and X C Zeng. Strain-dependent electronic and magnetic properties of MoS₂ monolayer, bilayer, nanoribbons and nanotubes. *Physical Chemistry Chemical Physics*, 14(37):13035–13040, 2012.
- ²⁰ R Ansari, S Malakpour, M Faghinasiri, and S Sahmani. An ab initio investigation into the elastic, structural and electronic properties of MoS₂ nanotubes. *Superlattices and Microstructures*, 82:188–200, 2015.
- ²¹ R Levi, J Garel, D Teich, G Seifert, R Tenne, and E Joselevich. Nanotube electromechanics beyond carbon: the case of WS₂. *ACS Nano*, 9(12):12224–12232, 2015.
- ²² A Bhardwaj, A Sharma, and P Suryanarayana. Torsional strain engineering of transition metal dichalcogenide nanotubes: An ab initio study. *Nanotechnology*, 32(47):47LT01, 2021.
- ²³ S Kumar and P Suryanarayana. Bending moduli for forty-four select atomic monolayers from first principles. *Nanotechnology*, 31(43):43LT01, 2020.
- ²⁴ A-Y Lu, H Zhu, J Xiao, C-P Chuu, Y Han, M-H Chiu, C-C Cheng, C-W Yang, K-H Wei, Y Yang, et al. Janus monolayers of transition metal dichalcogenides. *Nature Nanotechnology*, 12(8):744–749, 2017.
- ²⁵ J Zhang, S Jia, I Kholmanov, L Dong, D Er, W Chen, H Guo, Z Jin, V B Shenoy, L Shi, et al. Janus monolayer transition-metal dichalcogenides. *ACS Nano*, 11(8):8192–8198, 2017.
- ²⁶ D B Trivedi, G Turgut, Y Qin, M Y Sayyad, D Hajra, M Howell, L Liu, S Yang, N H Patoary, H Li, et al. Room-Temperature Synthesis of 2D Janus Crystals and their Heterostructures. *Advanced Materials*, 32(50):2006320, 2020.
- ²⁷ Y-C Lin, C Liu, Y Yu, E Zarkadoula, M Yoon, A A Puretzky, L Liang, Y Kong, Xand Gu, A Strasser, et al. Low energy implantation into transition-metal dichalcogenide monolayers to form Janus structures. *ACS Nano*, 14(4):3896–3906, 2020.
- ²⁸ Q-L Xiong, J Zhou, J Zhang, T Kitamura, and Z-H Li. Spontaneous curling of freestanding Janus monolayer transition-metal dichalcogenides. *Physical Chemistry Chemical Physics*, 20(32):20988–20995, 2018.
- ²⁹ Y Z Wang, R Huang, B L Gao, G Hu, F Liang, and Y L Ma. Mechanical and strain-tunable electronic properties of Janus MoSSe nanotubes. *Chalcogenide Letters*, 15(11):535–543, 2018.

- ³⁰ Z-K Tang, B Wen, M Chen, and L-M Liu. Janus MoSSe nanotubes: tunable band gap and excellent optical properties for surface photocatalysis. *Advanced Theory and Simulations*, 1(10):1800082, 2018.
- ³¹ AE G Mikkelsen, F T Bølle, K S Thygesen, T Vegge, and I E Castelli. Band structure of MoSTe Janus nanotubes. *Physical Review Materials*, 5(1):014002, 2021.
- ³² Y F Luo, Y Pang, M Tang, Q Song, and M Wang. Electronic properties of Janus MoSSe nanotubes. *Computational Materials Science*, 156:315–320, 2019.
- ³³ W Zhao, Y Li, W Duan, and F Ding. Ultra-stable small diameter hybrid transition metal dichalcogenide nanotubes X–M–Y (X, Y= S, Se, Te; M= Mo, W, Nb, Ta): a computational study. *Nanoscale*, 7(32):13586–13590, 2015.
- ³⁴ L Ju, P Liu, Y Yang, L Shi, G Yang, and L Sun. Tuning the photocatalytic water-splitting performance with the adjustment of diameter in an armchair WSSe nanotube. *Journal of Energy Chemistry*, 61:228–235, 2021.
- ³⁵ L Ju, J Qin, G Shi, Land Yang, J Zhang, and L Sun. Rolling the WSSe bilayer into double-walled nanotube for the enhanced photocatalytic water-splitting performance. *Nanomaterials*, 11(3):705, 2021.
- ³⁶ S Zhang, H Jin, C Long, T Wang, R Peng, B Huang, and Y Dai. MoSSe nanotube: a promising photocatalyst with an extremely long carrier lifetime. *Journal of Materials Chemistry A*, 7(13):7885–7890, 2019.
- ³⁷ S Xie, H Jin, Y Wei, and S Wei. Theoretical investigation on stability and electronic properties of Janus MoSSe nanotubes for optoelectronic applications. *Optik*, 227:166105, 2021.
- ³⁸ M. Yagmurcukardes, Y. Qin, S. Ozen, M. Sayyad, F. M. Peeters, S. Tongay and H. Sahin. Quantum properties and applications of 2D Janus crystals and their superlattices. *Applied Physics Reviews*, 7(1):011311, 2020.
- ³⁹ M Shtein, R Nadiv, N Lachman, H D Wagner, and O Regev. Fracture behavior of nanotube–polymer composites: Insights on surface roughness and failure mechanism. *Composites Science and Technology*, 87:157–163, 2013.
- ⁴⁰ G Otorgust, H Dodiuk, S Kenig, and R Tenne. Important insights into polyurethane nanocomposite-adhesives; a comparative study between INT-WS₂ and CNT. *European Polymer*

- Journal*, 89:281–300, 2017.
- ⁴¹ D M Simić, D B Stojanović, M Dimić, K Mišković, M Marjanović, Z Burzić, P S Uskoković, A Zak, and R Tenne. Impact resistant hybrid composites reinforced with inorganic nanoparticles and nanotubes of WS₂. *Composites Part B: Engineering*, 176:107222, 2019.
- ⁴² R Nadiv, M Shtein, M Refaeli, A Peled, and O Regev. The critical role of nanotube shape in cement composites. *Cement and Concrete Composites*, 71:166–174, 2016.
- ⁴³ S-J Huang, C-H Ho, Y Feldman, and R Tenne. Advanced AZ31 Mg alloy composites reinforced by WS₂ nanotubes. *Journal of Alloys and Compounds*, 654:15–22, 2016.
- ⁴⁴ M Naffakh, A M Diez-Pascual, and C Marco. Polymer blend nanocomposites based on poly (l-lactic acid), polypropylene and WS₂ inorganic nanotubes. *RSC Advances*, 6(46):40033–40044, 2016.
- ⁴⁵ D Yudilevich, R Levi, I Nevo, R Tenne, A Ya’akobovitz, and E Joselevich. Self-sensing torsional resonators based on inorganic nanotubes. *ICME*, pages 1–4, 2018.
- ⁴⁶ Y Divon, R Levi, J Garel, D Golberg, R Tenne, A Ya’akobovitz, and E Joselevich. Torsional resonators based on inorganic nanotubes. *Nano Letters*, 17(1):28–35, 2017.
- ⁴⁷ M Nath and C N R Rao. Nanotubes of group 4 metal disulfides. *Angewandte Chemie International Edition*, 41(18):3451–3454, 2002.
- ⁴⁸ A V Bandura and R A Evarestov. TiS₂ and ZrS₂ single-and double-wall nanotubes: First-principles study. *Journal of Computational Chemistry*, 35(5):395–405, 2014.
- ⁴⁹ Felix T Bülle, A E G Mikkelsen, K S Thygesen, T Vegge, and I E Castelli. Structural and chemical mechanisms governing stability of inorganic Janus nanotubes. *npj Computational Materials*, 7(1):1–8, 2021.
- ⁵⁰ A Sharma and P Suryanarayana. Real-space density functional theory adapted to cyclic and helical symmetry: Application to torsional deformation of carbon nanotubes. *Physical Review B*, 103(3):035101, 2021.
- ⁵¹ Q Xu, A Sharma, B Comer, H Huang, E Chow, A J Medford, J E Pask, and P Suryanarayana. Sparc: Simulation package for ab-initio real-space calculations. *SoftwareX*, 15:100709, 2021.
- ⁵² S Ghosh and P Suryanarayana. SPARC: Accurate and efficient finite-difference formulation and parallel implementation of density functional theory: Isolated clusters. *Computer Physics*

- Communications*, 212:189–204, 2017.
- ⁵³ S Ghosh and P Suryanarayana. SPARC: Accurate and efficient finite-difference formulation and parallel implementation of Density Functional Theory: Extended systems. *Computer Physics Communications*, 216:109–125, 2017.
- ⁵⁴ S Ghosh, A S Banerjee, and P Suryanarayana. Symmetry-adapted real-space density functional theory for cylindrical geometries: Application to large group-IV nanotubes. *Physical Review B*, 100(12):125143, 2019.
- ⁵⁵ A S Banerjee and P Suryanarayana. Cyclic density functional theory: A route to the first principles simulation of bending in nanostructures. *Journal of the Mechanics and Physics of Solids*, 96:605–631, 2016.
- ⁵⁶ A S Banerjee, L Lin, P Suryanarayana, C Yang, and J E Pask. Two-level Chebyshev filter based complementary subspace method: pushing the envelope of large-scale electronic structure calculations. *Journal of Chemical Theory and Computation*, 14(6):2930–2946, 2018.
- ⁵⁷ David Codony, Irene Arias, and Phanish Suryanarayana. Transversal flexoelectric coefficient for nanostructures at finite deformations from first principles. *Physical Review Materials*, 5(3):L030801, 2021.
- ⁵⁸ S Kumar, D Codony, I Arias, and P Suryanarayana. Flexoelectricity in atomic monolayers from first principles. *Nanoscale*, 13(3):1600–1607, 2021.
- ⁵⁹ K Momma and F Izumi. VESTA: a three-dimensional visualization system for electronic and structural analysis. *Journal of Applied Crystallography*, 41(3):653–658, 2008.
- ⁶⁰ M. F. Shojaei, J. E. Pask, A. J. Medford, and P. Suryanarayana. Soft and transferable pseudopotentials from multi-objective optimization. *arXiv preprint arXiv:2209.09806*, 2022.
- ⁶¹ D R Hamann. Optimized norm-conserving Vanderbilt pseudopotentials. *Physical Review B*, 88(8):085117, 2013.
- ⁶² W Shi and Z Wang. Mechanical and electronic properties of Janus monolayer transition metal dichalcogenides. *Journal of Physics: Condensed Matter*, 30(21):215301, 2018.
- ⁶³ J P Perdew, K Burke, and M Ernzerhof. Generalized gradient approximation made simple. *Physical Review Letters*, 77(18):3865, 1996.

- ⁶⁴ Y Z Wang, R Huang, X Q Wang, Q F Zhang, B L Gao, L Zhou, and G Hua. Strain-tunable electronic properties of CrS₂ nanotubes. *Chalcogenide Letters*, 13(7):301–307, 2016.
- ⁶⁵ J Xiao, M Long, X Li, H Xu, H Huang, and Y Gao. Theoretical prediction of electronic structure and carrier mobility in single-walled MoS₂ nanotubes. *Scientific Reports*, 4(1):1–7, 2014.
- ⁶⁶ C Ataca, H Sahin, and S Ciraci. Stable, single-layer MX₂ transition-metal oxides and dichalcogenides in a honeycomb-like structure. *The Journal of Physical Chemistry C*, 116(16):8983–8999, 2012.
- ⁶⁷ C-H Chang, X Fan, S-H Lin, and J-L Kuo. Orbital analysis of electronic structure and phonon dispersion in MoS₂, MoSe₂, WS₂, and WSe₂ monolayers under strain. *Physical Review B*, 88(19):195420, 2013.
- ⁶⁸ B Amin, T P Kaloni, and U Schwingenschlögl. Strain engineering of WS₂, WSe₂, and WTe₂. *RSC Advances*, 4(65):34561–34565, 2014.
- ⁶⁹ H Guo, N Lu, L Wang, X Wu, and X C Zeng. Tuning electronic and magnetic properties of early transition-metal dichalcogenides via tensile strain. *The Journal of Physical Chemistry C*, 118(13):7242–7249, 2014.
- ⁷⁰ J Chen, S-L Li, Z-L Tao, Y-T Shen, and C-X Cui. Titanium disulfide nanotubes as hydrogen-storage materials. *Journal of the American Chemical Society*, 125(18):5284–5285, 2003.
- ⁷¹ M Nath, S Kar, A K Raychaudhuri, and C N R Rao. Superconducting NbSe₂ nanostructures. *Chemical Physics Letters*, 368(5-6):690–695, 2003.
- ⁷² M Nath and C N R Rao. MoSe₂ and WSe₂ nanotubes and related structures. *Chemical Communications*, 1(21):2236–2237, 2001.
- ⁷³ A R Klots, A K M Newaz, B Wang, D Prasai, H Krzyzanowska, J Lin, D Caudel, N J Ghimire, J Yan, B L Ivanov, et al. Probing excitonic states in suspended two-dimensional semiconductors by photocurrent spectroscopy. *Scientific Reports*, 4(1):1–7, 2014.
- ⁷⁴ M M Ugeda, A J Bradley, S-F Shi, H Felipe, Y Zhang, D Y Qiu, W Ruan, S-K Mo, Z Hussain, Z-X Shen, et al. Giant bandgap renormalization and excitonic effects in a monolayer transition metal dichalcogenide semiconductor. *Nature Materials*, 13(12):1091–1095, 2014.
- ⁷⁵ H M Hill, A F Rigosi, K T Rim, G W Flynn, and T F Heinz. Band alignment in MoS₂/WS₂ transition metal dichalcogenide heterostructures probed by scanning tunneling microscopy and

- spectroscopy. *Nano Letters*, 16(8):4831–4837, 2016.
- ⁷⁶ Kostya S Novoselov, D Jiang, F Schedin, TJ Booth, VV Khotkevich, SV Morozov, and Andre K Geim. Two-dimensional atomic crystals. *Proceedings of the National Academy of Sciences*, 102(30):10451–10453, 2005.
- ⁷⁷ Jonathan N Coleman, Mustafa Lotya, Arlene O’Neill, Shane D Bergin, Paul J King, Umar Khan, Karen Young, Alexandre Gaucher, Sukanta De, Ronan J Smith, et al. Two-dimensional nanosheets produced by liquid exfoliation of layered materials. *Science*, 331(6017):568–571, 2011.
- ⁷⁸ K S Nagapriya, O Goldbart, I Kaplan-Ashiri, G Seifert, R Tenne, and E Joselevich. Torsional stick-slip behavior in WS₂ nanotubes. *Physical Review Letters*, 101(19):195501, 2008.
- ⁷⁹ Yonggang Huang, J Wu, and Keh-Chih Hwang. Thickness of graphene and single-wall carbon nanotubes. *Physical Review B*, 74(24):245413, 2006.
- ⁸⁰ M M Jubbessen Treacy, Thomas W Ebbesen, and John M Gibson. Exceptionally high Young’s modulus observed for individual carbon nanotubes. *Nature*, 381(6584):678–680, 1996.
- ⁸¹ T C T Ting and T Chen. Poisson’s ratio for anisotropic elastic materials can have no bounds. *The Quarterly Journal of Mechanics and Applied Mathematics*, 58(1):73–82, 2005.